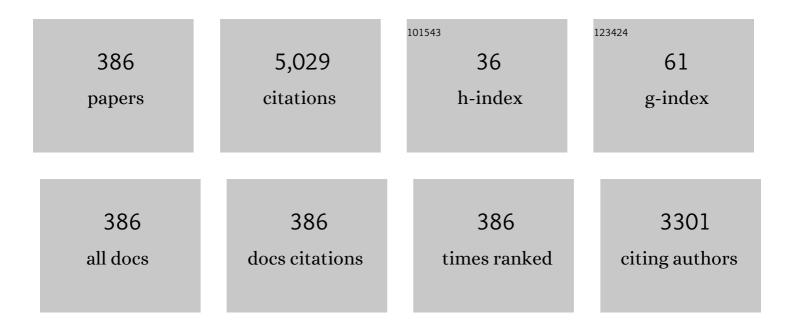
Tomas Mocek

List of Publications by Year in descending order

Source: https://exaly.com/author-pdf/6973157/publications.pdf Version: 2024-02-01



TOMAS MOCEK

#	Article	IF	CITATIONS
1	The effect of laser shock peening with and without protective coating on intergranular corrosion of sensitized AA5083. Corrosion Science, 2022, 194, 109925.	6.6	20
2	Spectral broadening and a prospect for pulse compression of Yb:YAG thin-disk laser pulses by nonlinear SHG in a BBO crystal with time predelay and tilting of the pulse fronts. , 2022, 1, 16.		0
3	Investigation of the lasing performance of a crystalline-coated Yb:YAG thin-disk directly bonded onto a silicon carbide heatsink. Optics Express, 2022, 30, 7708.	3.4	5
4	Analysis of broadband mid-infrared optical parametric amplification based on LiGaS ₂ , LiGaSe ₂ , LiInS ₂ , and LiInSe ₂ crystals. Journal of the Optical Society of America B: Optical Physics, 2022, 39, 1174.	2.1	1
5	Qualification of 1030 nm ultra-short-pulsed laser for glass sheet treatment in TGV process. , 2022, , .		Ο
6	Fatigue life enhancement of additive manufactured 316l stainless steel by LSP using a DPSS laser system. Surface Engineering, 2022, 38, 183-190.	2.2	14
7	Morphology of Meteorite Surfaces Ablated by High-Power Lasers: Review and Applications. Applied Sciences (Switzerland), 2022, 12, 4869.	2.5	2
8	Difference Frequency Generation in BaGa4Se7 Tunable in a 6.5-8.5 μm Range with a Peak Power of 30 MW Pumped by 1.03 μm, 1.8 ps Laser. , 2022, , .		1
9	Diode pumped cryogenic Yb:Lu3Al5O12 laser in continuous-wave and pulsed regime. Optics and Laser Technology, 2021, 135, 106720.	4.6	6
10	Monoclinic zinc monotungstate Yb3+,Li+:ZnWO4: Part II. Polarized spectroscopy and laser operation. Journal of Luminescence, 2021, 231, 117811.	3.1	5
11	Diode-pumped, electro-optically <i>Q</i> -switched, cryogenic Tm:YAG laser operating at 1.88 μm. High Power Laser Science and Engineering, 2021, 9, .	4.6	7
12	Silicon Brewster plate wavelength separator for a mid-IR optical parametric source. Applied Optics, 2021, 60, 281.	1.8	1
13	Laser Annealing of Anodic TiO2 Nanotubes: Explosive Solid Phase Crystallization into Anatase. , 2021, , .		Ο
14	Picosecond thin-disk laser platform PERLA for multi-beam micromachining. OSA Continuum, 2021, 4, 940.	1.8	17
15	Anti-Reflection Nanostructures on Tempered Glass by Dynamic Beam Shaping. Micromachines, 2021, 12, 289.	2.9	9
16	Diode-pumped master oscillator power amplifier system based on cryogenically cooled Tm:Y2O3 transparent ceramics. Optical Materials Express, 2021, 11, 1489.	3.0	4
17	Compact, diode-pumped, unstable cavity Yb:YAG laser and its application in laser shock peening. Optics Express, 2021, 29, 15724.	3.4	2
18	Picosecond VIS, UV and Deep UV Beams Generated at 100 kHz Diode-Pumped Yb:YAG Thin Disk Laser System. , 2021, , .		0

#	ARTICLE	IF	CITATIONS
19	2 μm MOPA Laser Based on Cryogenically Cooled Tm:Y2O3 Transparent Ceramic. , 2021, , .		0
20	Towards Rapid Fabrication of Superhydrophobic Surfaces by Multi-Beam Nanostructuring with 40,401 Beams. Nanomaterials, 2021, 11, 1987.	4.1	8
21	150 J DPSSL operating at 1.5 kW level. Optics Letters, 2021, 46, 5771.	3.3	32
22	Influence of the CVBG compressor on output parameters of high-power and high-energy laser beam. , 2021, , .		0
23	Lasing performance of crystalline-coated Yb:YAG thin disks. , 2021, , .		1
24	Hydrophilic to ultrahydrophobic transition of Al 7075 by affordable ns fiber laser and vacuum processing. Applied Surface Science, 2020, 505, 144523.	6.1	41
25	Fabrication of functional superhydrophobic surfaces on carbon fibre reinforced plastics by IR and UV direct laser interference patterning. Applied Surface Science, 2020, 508, 144817.	6.1	20
26	Faraday Rotation of Dy2O3, CeF3 and Y3Fe5O12 at the Mid-Infrared Wavelengths. Materials, 2020, 13, 5324.	2.9	18
27	Micromachining of Invar with 784 Beams Using 1.3 ps Laser Source at 515 nm. Materials, 2020, 13, 2962.	2.9	14
28	Large-Beam Picosecond Interference Patterning of Metallic Substrates. Materials, 2020, 13, 4676.	2.9	13
29	Laser-induced crystallization of anodic TiO ₂ nanotube layers. RSC Advances, 2020, 10, 22137-22145.	3.6	23
30	Spectroscopy and diode-pumped continuous-wave laser operation of Tm:Y2O3 transparent ceramic at cryogenic temperatures. Applied Physics B: Lasers and Optics, 2020, 126, 1.	2.2	10
31	Experimental Study of Nanosecond Laser-Generated Plasma Channels. Applied Sciences (Switzerland), 2020, 10, 4082.	2.5	1
32	Balancing the conversion efficiency and beam quality of second harmonic generation of a two-picosecond Yb:YAG thin-disk laser. Laser Physics, 2020, 30, 025405.	1.2	7
33	Investigation of spectrally-dependent phonon relaxation mechanism in Yb:YAG gain media and its consequences for thin disk laser performance. Laser Physics, 2020, 30, 025005.	1.2	1
34	Experimental study on compression of 216-W laser pulses below 2  ps at 1030  nm with chirpe Bragg grating. Applied Optics, 2020, 59, 7938.	d yolume 1.8	10
35	Numerical analysis of beam distortion induced by thermal effects in chirped volume Bragg grating compressors for high-power lasers. Journal of the Optical Society of America B: Optical Physics, 2020, 37, 3874.	2.1	5
36	Performance comparison of Yb:YAG ceramics and crystal gain material in a large-area, high-energy, high average–power diode-pumped laser. Optics Express, 2020, 28, 3636.	3.4	11

#	Article	IF	CITATIONS
37	Spectroscopy and diode-pumped laser operation of transparent Tm:Lu ₃ Al ₅ O ₁₂ ceramics produced by solid-state sintering. Optics Express, 2020, 28, 28399.	3.4	6
38	Verdet constant of potassium terbium fluoride crystal as a function of wavelength and temperature. Optics Letters, 2020, 45, 1683.	3.3	19
39	Multi-watt continuous-wave and passively Q-switched Tm:CaYAlO4 micro-lasers. , 2020, , .		0
40	Shaping of picosecond laser pulses by second harmonic generation with time predelay. , 2020, , .		1
41	Tensor-to-matrix mapping in elasto-optics. Journal of the Optical Society of America B: Optical Physics, 2020, 37, 1090.	2.1	3
42	Multiple pulse picosecond laser induced damage threshold on hybrid mirrors. , 2020, , .		0
43	Numerical study of sum frequency ultrashort pulse compression in borate crystals. Journal of the Optical Society of America B: Optical Physics, 2020, 37, 3229.	2.1	2
44	Verdet Constant of Magneto-Active Materials Developed for High-Power Faraday Devices. Applied Sciences (Switzerland), 2019, 9, 3160.	2.5	77
45	Numerical Analysis of Thermal Effects in a Concept of a Cryogenically Cooled Yb: YAG Multislab 10 J/100-Hz Laser Amplifier. IEEE Journal of Quantum Electronics, 2019, 55, 1-8.	1.9	5
46	Efficient diode pumped Yb:Y2O3 cryogenic laser. Applied Physics B: Lasers and Optics, 2019, 125, 1.	2.2	7
47	Non-fluorinated superhydrophobic Al7075 aerospace alloy by ps laser processing. Applied Surface Science, 2019, 493, 287-293.	6.1	53
48	Single Shot M2 Measurement for Near Infrared Laser Pulses in Real-Time. , 2019, , .		0
49	Picosecond Deep Ultraviolet Pulses Generated in Excess of the 1030 nm Fundamental Beam. , 2019, , .		0
50	Characterization of the Verdet Constant of Dy2O3 Ceramics in the Two-Micron Spectral Range. , 2019, , \cdot		0
51	Nanostructure fabrication on the top of laser-made micropillars for enhancement of water repellence of aluminium alloy. Materials Letters, 2019, 256, 126601.	2.6	19
52	LIPSS on thin metallic films: New insights from multiplicity of laser-excited electromagnetic modes and efficiency of metal oxidation. Applied Surface Science, 2019, 491, 650-658.	6.1	50
53	Generating 84 fs, 4 nJ directly from an Yb-doped fiber oscillator by optimization of the net dispersion. Laser Physics, 2019, 29, 065105.	1.2	2
54	A high-brightness room temperature 2.7 <i>µ</i> m Er:Y ₂ O ₃ ceramic laser. Laser Physics Letters, 2019, 16, 035801.	1.4	8

#	Article	IF	CITATIONS
55	Peak Power Enhancement of Yb:YAG Laser Pulses by Second Harmonic Generation with Time Predelay in Borate Crystals. , 2019, , .		0
56	Dependencies of Picosecond Pulse Driven Supercontinuum Properties on Repetition Rate. , 2019, , .		0
57	Diode $\hat{a} \in \mathbb{C}$ Pumped Efficient Cryogenic Yb:Y2O3 Transparent Ceramic Laser. , 2019, , .		0
58	Spectroscopy, Continuous-Wave and Passively Q-Switched Laser Operation of Transparent Tm:LuAG Ceramics. , 2019, , .		0
59	Spectroscopy of Tm:Y2O3 Transparent Ceramic at Cryogenic Temperatures. , 2019, , .		0
60	Development of a High-Quality Epoxy Bonding Technology. , 2019, , .		0
61	Effect of Gd3+/Ga3+ on Yb3+ emission in mixed YAG at cryogenic temperature. Ceramics International, 2019, 45, 9418-9422.	4.8	5
62	Characteristics of a high-power picosecond mid-IR parametric generator/amplifier tunable between 1.5 and 3.2 μm. , 2019, , .		3
63	Design of a 10 J, 100 Hz diode-pumped solid state laser. , 2019, , .		2
64	Novel unstable resonator configuration for highly efficient cryogenically cooled Yb:YAG Q-switched laser. Optics Express, 2019, 27, 21622.	3.4	8
65	New observations on DUV radiation at 257â€nm and 206â€nm produced by a picosecond diode pumped thin-disk laser. Optics Express, 2019, 27, 24286.	3.4	21
66	Temperature-wavelength dependence of Verdet constant of Dy ₂ O ₃ ceramics. Optical Materials Express, 2019, 9, 2971.	3.0	28
67	Laser performances of diode pumped Yb:Lu ₂ O ₃ transparent ceramic at cryogenic temperatures. Optical Materials Express, 2019, 9, 4669.	3.0	8
68	Synthesis, Spectroscopy and Efficient Laser Operation of Tm:Lu3Al5O12 Transparent Ceramics. , 2019, , .		0
69	Concepts for Adapting Highly Efficient Diode Pumped Laser Technology for Laser Shock Peening. , 2019, , .		Ο
70	Thermo-optical Study of 10 J/ 100 Hz Cryogenically Cooled Yb:YAG Diode Pumped Laser System. , 2019, , .		0
71	Picosecond deep ultraviolet pulses generated by a 100 kHz thin-disk laser system. , 2019, , .		2
72	Importance of Laser Induced Damage Threshold for Laser Applications. , 2019, , .		0

#	Article	IF	CITATIONS
73	Highly efficient, cryogenically cooled Yb:YAG q-switch laser based on a gain modulated unstable resonator design. , 2019, , .		0
74	Monocrystalline materials for high-power ultrafast lasers. , 2019, , .		0
75	Diode-pumped cryogenic Tm:LiYF4 laser. , 2019, , .		1
76	Single-shot laser beam parameter measurement system for near-infrared laser beams. Journal of the Optical Society of America B: Optical Physics, 2019, 36, 3098.	2.1	0
77	Comparison of multipulse nanosecond LIDT of HR coated YAG and glass substrates at 1030 nm. , 2019, , .		0
78	Mobile LIDT. , 2019, , .		0
79	Modular laser beam distribution system for the HiLASE Center. , 2019, , .		Ο
80	EUV SOURCE AT HILASE: THE STATE OF THE ART. MM Science Journal, 2019, 2019, 3406-3409.	0.4	0
81	Highly Efficient, Compact Tm3+:RE2O3 (RE = Y, Lu, Sc) Sesquioxide Lasers Based on Thermal Guiding. IEEE Journal of Selected Topics in Quantum Electronics, 2018, 24, 1-13.	2.9	40
82	Faraday effect measurements of holmium oxide (Ho ₂ O ₃) ceramics-based magneto-optical materials. High Power Laser Science and Engineering, 2018, 6, .	4.6	28
83	Crystal growth, low-temperature spectroscopy and multi-watt laser operation of Yb:Ca3NbGa3Si2O14. Journal of Luminescence, 2018, 197, 90-97.	3.1	9
84	Overview of ytterbium based transparent ceramics for diode pumped high energy solid-state lasers. High Power Laser Science and Engineering, 2018, 6, .	4.6	14
85	Passive Q switching of Yb:CNGS lasers by Cr ⁴⁺ :YAG and V ³⁺ :YAG saturable absorbers. Applied Optics, 2018, 57, 8236.	1.8	2
86	Initiation of air ionization by ultrashort laser pulses: evidence for a role of metastable-state air molecules. Journal Physics D: Applied Physics, 2018, 51, 25LT02.	2.8	9
87	Spectroscopic investigations of thulium doped YAG and YAP crystals between 77â€⁻K and 300â€⁻K for short-wavelength infrared lasers. Journal of Luminescence, 2018, 202, 427-437.	3.1	26
88	Efficient diode-pumped Er:KLu(WO_4)_2 laser at â^¼161  μm. Optics Letters, 2018, 43, 218.	3.3	6
89	Femtosecond 85  μm source based on intrapulse difference-frequency generation of 21  μm Letters, 2018, 43, 1335.	pulses. C	Optics
90	Femtosecond Yb:YGAG ceramic slab regenerative amplifier. Optical Materials Express, 2018, 8, 615.	3.0	8

#	Article	IF	CITATIONS
91	High power picosecond parametric mid-IR source tunable between 17 and 26  μm. Applied Optics, 2018 8412.	8,57, 1.8	5
92	High Power Picosecond Parametric Mid-IR Source Tunable Between 1.5 and 3.2 Î $^1\!\!/4$ m. , 2018, , .		1
93	Fs-laser-written erbium-doped double tungstate waveguide laser. Optics Express, 2018, 26, 30826.	3.4	9
94	High-Energy Burst Mode Thin-disk Multipass Amplifier for Laser Compton X-ray Source. , 2018, , .		1
95	Large Scale Single Crystal Growth. , 2018, , .		0
96	A Femtosecond 8.5 μm Source Based on Intrapulse Difference-Frequency Generation of 2.1 μm Pulses. , 2018, , .		0
97	Development of experimental station for laser shock peening at HiLASE. , 2018, , .		0
98	100J-level nanosecond pulsed Yb:YAG cryo-cooled DPSSL amplifier. , 2018, , .		1
99	Ten-watt level picosecond parametric mid-IR source broadly tunable in wavelength. , 2018, , .		0
100	Characterization of Bivoj/DiPOLE 100: HiLASE 100-J/10-Hz diode pumped solid state laser. , 2018, , .		3
101	Generation of 1-J bursts with picosecond pulses from Perla B thin-disk laser system. , 2018, , .		0
102	Wavefront correction with photo-controlled deformable mirror. , 2018, , .		0
103	High-energy subpicosecond 2.1-um fiber laser. , 2018, , .		0
104	HILASE center: development of new-generation lasers for laser shock peening. , 2018, , .		1
105	Laser induced damage in optical glasses using nanosecond pulses at 1030 nm. , 2018, , .		0
106	Multiple pulse nanosecond laser-induced damage threshold on AR coated YAG crystals. , 2018, , .		1
107	A 100J-level nanosecond pulsed DPSSL for pumping high-efficiency, high-repetition rate PW-class lasers. Proceedings of SPIE, 2017, , .	0.8	3
108	Lasing and thermal characteristics of Yb:YAG/YAG composite with atomic diffusion bonding. Laser Physics Letters, 2017, 14, 015001.	1.4	21

#	Article	IF	CITATIONS
109	Investigation and modelling of pump saturation effect on thermal load of Yb:YAG thin disk pumped at various wavelengths. Proceedings of SPIE, 2017, , .	0.8	0
110	A 100 J-level nanosecond DPSSL for high energy density experiments. Proceedings of SPIE, 2017, , .	0.8	1
111	Commissioning of a kW-class nanosecond pulsed DPSSL operating at 105 J, 10 Hz. Proceedings of SPIE, 2017, , .	0.8	2
112	Laser-induced periodic surface structures formation: investigation of the effect of nonlinear absorption of laser energy in different materials. Proceedings of SPIE, 2017, , .	0.8	7
113	Wavefront aberration measurement in a cryogenically cooled Yb:YAG slab using a wavefront sensor. , 2017, , .		1
114	Temperature dependent spectroscopic characterization of Tm:YAG crystals as potential laser medium for pulsed high energy laser amplifiers. , 2017, , .		1
115	Development of 2.7-μm Er:Y2O ₃ ceramic laser operated at room temperature. Proceedings of SPIE, 2017, , .	0.8	Ο
116	Verdet constant dispersion of CeF ₃ in the visible and near-infrared spectral range. Optical Engineering, 2017, 56, 067105.	1.0	15
117	High-speed manufacturing of highly regular femtosecond laser-induced periodic surface structures: physical origin of regularity. Scientific Reports, 2017, 7, 8485.	3.3	251
118	Demonstration of laser oscillation of an Yb-doped Y <inf>2</inf> O <inf>3</inf> composite disk by use of atomic diffusion bonding in room temperature. , 2017, , .		0
119	The first kilowatt average power 100J-level DPSSL. , 2017, , .		Ο
120	HiLASE: New lasers for industry and research. , 2017, , .		0
121	How new laser development can help laser shock peening penetration to widen industrial applications?. , 2017, , .		4
122	Continuous-wave and passively Q-switched cryogenic Yb:KLu(WO_4)_2 laser. Optics Express, 2017, 25, 25886.	3.4	4
123	Cryogenic Yb:YGAG ceramic laser pumped at 940 nm and zero-phonon-line: a comparative study. Optical Materials Express, 2017, 7, 477.	3.0	Ο
124	Kilowatt average power 100  J-level diode pumped solid state laser. Optica, 2017, 4, 438.	9.3	152
125	Advances in High-Power, Ultrashort Pulse DPSSL Technologies at HiLASE. Applied Sciences (Switzerland), 2017, 7, 1016.	2.5	42
126	kW-class picosecond and nanosecond lasers at Hilase for hi-tech industrial applications. , 2017, , .		0

8

#	Article	IF	CITATIONS
127	The first multi-joule DPSSL with 1 kW average power. , 2017, , .		0
128	kW-class picosecond thin-disc prepulse laser Perla for efficient EUV generation. Journal of Micro/ Nanolithography, MEMS, and MOEMS, 2017, 16, 1.	0.9	3
129	Microchip Yb:CaLnAlO_4 lasers with up to 91% slope efficiency. Optics Letters, 2017, 42, 2431.	3.3	57
130	Wavelength Tunable Picosecond Parametric Mid-IR Source Pumped by a High Power Thin-Disk Laser. , 2017, , .		0
131	Diode-pumped femtosecond Yb:YGAG regenerative amplifier. , 2017, , .		0
132	Wavelength tunable parametric mid-IR source pumped by a high power picosecond thin-disk laser. , 2017, , .		0
133	Multiple pulse nanosecond laser induced damage threshold on hybrid mirrors. , 2017, , .		2
134	A practical model of thin disk regenerative amplifier based on analytical expression of ASE lifetime. , 2017, , .		0
135	Laser beam distribution system for the HiLASE Center. , 2017, , .		1
136	Temperature-wavelength dependence of terbium gallium garnet ceramics Verdet constant. Optical Materials Express, 2016, 6, 3683.	3.0	63
137	Picosecond green and deep ultraviolet pulses generated by a high-power 100  kHz thin-disk laser. Optics Letters, 2016, 41, 5210.	3.3	26
138	Innovative opto-mechanical design of a laser head for compact thin-disk. Proceedings of SPIE, 2016, , .	0.8	0
139	Mechanisms of high-regularity periodic structuring of silicon surface by sub-MHz repetition rate ultrashort laser pulses. Applied Physics Letters, 2016, 109, .	3.3	56
140	Laser induced damage threshold of optical fibers under ns pulses. Proceedings of SPIE, 2016, , .	0.8	1
141	Design of deformable mirrors for high power lasers. High Power Laser Science and Engineering, 2016, 4, .	4.6	10
142	Ultrashort pulse laser ablation of dielectrics: Thresholds, mechanisms, role of breakdown. Scientific Reports, 2016, 6, 39133.	3.3	110
143	HiLASE: a scalable option for Laser Inertial Fusion Energy. Journal of Physics: Conference Series, 2016, 688, 012060.	0.4	1
144	Time-resolved measurement of thermally induced aberrations in a cryogenically cooled Yb:YAG slab with a wavefront sensor. Applied Physics B: Lasers and Optics, 2016, 122, 1.	2.2	4

#	Article	IF	CITATIONS
145	Microchip laser operation of Yb-doped gallium garnets. Optical Materials Express, 2016, 6, 46.	3.0	31
146	Comparative LIDT measurements of optical components for high-energy HiLASE lasers. High Power Laser Science and Engineering, 2016, 4, .	4.6	11
147	Cryogenic Yb:YAG Laser Pumped by VBC-Stabilized Narrowband Laser Diode at 969 nm. IEEE Photonics Technology Letters, 2016, 28, 1328-1331.	2.5	14
148	3-D Particle-in-Cell Simulation of Laser-Produced Plasma in Axial Magnetic Field. IEEE Transactions on Plasma Science, 2016, 44, 574-581.	1.3	3
149	Design of an Optimized Adaptive Optics System With a Photo-Controlled Deformable Mirror. IEEE Photonics Technology Letters, 2016, 28, 1422-1425.	2.5	3
150	Picosecond pulses in deep ultraviolet (257.5 nm and 206 nm) and mid-IR produced by a high-power 100 kHz solid-state thin-disk laser. Proceedings of SPIE, 2016, , .	0.8	1
151	Development of a kW-level picosecond thin-disk regenerative amplifier with a ring cavity. , 2016, , .		0
152	100  J-level nanosecond pulsed diode pumped solid state laser. Optics Letters, 2016, 41, 2089.	3.3	73
153	Zero-phonon-line pumped cryogenic Yb:YAG passively Q-switched by Cr:YAG. Proceedings of SPIE, 2016, , .	0.8	0
154	Cryogenically-cooled Yb:YGAG ceramic picosecond oscillator. Proceedings of SPIE, 2016, , .	0.8	0
155	Relaxation dynamics of femtosecond-laser-induced temperature modulation on the surfaces of metals and semiconductors. Applied Surface Science, 2016, 374, 157-164.	6.1	72
156	Diode pumped compact cryogenic Yb:YAG/Cr:YAG pulsed laser. Proceedings of SPIE, 2016, , .	0.8	4
157	Progress in kW-class picosecond thin-disk lasers development at the HiLASE. Proceedings of SPIE, 2016,	0.8	5
158	Ultrashort-pulse laser processing of transparent materials: insight from numerical and semi-analytical models. Proceedings of SPIE, 2016, , .	0.8	7
159	Cryogenically-cooled Yb:YGAG ceramic mode-locked laser. Optics Express, 2016, 24, 1402.	3.4	6
160	Parametric Mid-IR Source Pumped by a High Power Picosecond Thin-Disk Laser. , 2016, , .		0
161	A 100J-level nanosecond pulsed DPSSL. , 2016, , .		1
162	Development of short pulse CO2 laser for efficient rare earth plasma extreme ultraviolet sources. , 2015, , .		0

#	Article	IF	CITATIONS
163	Laser fluence dependence of periodic structures on metals produced by femtosecond double pulse laser. , 2015, , .		0
164	Status of the High Average Power Diode-Pumped Solid State Laser Development at HiLASE. Applied Sciences (Switzerland), 2015, 5, 637-665.	2.5	65
165	EUV ablation: a study of the process. , 2015, , .		2
166	Cooling options for high-average-power laser mirrors. , 2015, , .		1
167	Experimental benchmarking of the code for Yb:YAG multi-slab gas-cooled laser system operating at cryogenic temperatures. , 2015, , .		0
168	Picosesond pulses in deep ultraviolet produced by a 100 kHz solid-state thin disk laser. Proceedings of SPIE, 2015, , .	0.8	0
169	Temperature dependent absorption measurement of various transition metal doped laser materials. Proceedings of SPIE, 2015, , .	0.8	2
170	Amplification of picosecond pulses to 100 W by an Yb:YAG thin-disk with CVBG compressor. , 2015, , .		9
171	Joule-class 940 nm diode laser bars for millisecond pulse applications. , 2015, , .		0
172	How to optimize ultrashort pulse laser interaction with glass surfaces in cutting regimes?. Applied Surface Science, 2015, 336, 364-374.	6.1	35
173	Wavelength tunability of laser based on Yb-doped YGAG ceramics. , 2015, , .		2
174	First experimental test of quadrupole lens-free multiple profile monitor technique for electron beam emittance measurement with a PW laser system. Proceedings of SPIE, 2015, , .	0.8	0
175	Single shot M ² measurement for near infrared high energy laser pulses. Proceedings of SPIE, 2015, , .	0.8	Ο
176	Thermally induced depolarization in terbium gallium garnet ceramics rod with natural convection cooling. Journal of Optics (United Kingdom), 2015, 17, 065610.	2.2	8
177	Laser-induced ion acceleration at ultra-high laser intensities. Radiation Effects and Defects in Solids, 2015, 170, 271-277.	1.2	3
178	Assessment of high-power kW-class single-diode bars for use in highly efficient pulsed solid state laser systems. , 2015, , .		0
179	Design and development of the HELL user station: beam transport, characterization, and shielding. , 2015, , .		1
180	Timing jitter measurement and stabilization of a mode-locked ytterbium fiber laser. Proceedings of SPIE, 2015, , .	0.8	0

#	Article	IF	CITATIONS
181	Precise curvature measurement of Yb:YAG thin disk. , 2015, , .		4
182	Focal spot of femtosecond laser pulse under tight focusing condition. Proceedings of SPIE, 2015, , .	0.8	0
183	Experimental and theoretical study of deformable mirror actuator arrays. Proceedings of SPIE, 2015, , .	0.8	0
184	Wavefront control in high average-power multi-slab laser system. , 2015, , .		1
185	HiLASE Project: high intensity lasers for industrial and scientific applications. , 2015, , .		0
186	Tunable diode laser absorption spectroscopy on 2.05 \hat{l} /4m for the CO ₂ concentration measurement. Proceedings of SPIE, 2015, , .	0.8	0
187	Periodic surface structures on titanium self-organized upon double femtosecond pulse exposures. Applied Surface Science, 2015, 336, 349-353.	6.1	29
188	Formation of laser induced periodic surface structures (LIPSS) on Ti upon double fs pulse exposure. , 2015, , .		0
189	Development of a closed-loop cryogenically cooled sub-picosecond regenerative amplifier. , 2015, , .		0
190	HiLASE: development of fully diode pumped disk lasers with high average power. , 2015, , .		1
191	Collimation of laser-produced plasmas using axial magnetic field. Laser and Particle Beams, 2015, 33, 175-182.	1.0	25
192	Graphene Q-Switched Compact Yb:YAG Laser. IEEE Photonics Journal, 2015, 7, 1-7.	2.0	15
193	Wavelength dependence of magneto-optic properties of terbium gallium garnet ceramics. Optics Express, 2015, 23, 13641.	3.4	42
194	1-J operation of monolithic composite ceramics with Yb:YAG thin layers: multi-TRAM at 10-Hz repetition rate and prospects for 100-Hz operation. Optics Letters, 2015, 40, 855.	3.3	24
195	Spatio-temporal modification of femtosecond focal spot under tight focusing condition. Optics Express, 2015, 23, 11641.	3.4	31
196	Spectroscopic and lasing characteristics of Yb:YGAG ceramic at cryogenic temperatures. Optical Materials Express, 2015, 5, 1289.	3.0	19
197	Recent Advances on the J-KAREN laser upgrade. , 2015, , .		0
198	Time-resolved deformation measurement of Yb:YAG thin disk using wavefront sensor. Proceedings of SPIE, 2015, , .	0.8	1

#	Article	IF	CITATIONS
199	Joule-Class 940-nm Diode Laser Bars for Millisecond Pulse Applications. IEEE Photonics Technology Letters, 2015, 27, 1663-1666.	2.5	7
200	New possibilities for efficient laser surface treatment by diodeâ€pumped kWâ€class lasers. Journal of Engineering, 2015, 2015, 158-160.	1.1	1
201	Continuous-wave seeded mid-IR parametric system pumped by the high-average-power picosecond Yb:YAG thin-disk laser. Proceedings of SPIE, 2015, , .	0.8	1
202	Efficient laser performance of a cryogenic Yb:YAG laser pumped by fiber coupled 940 and 969 nm laser diodes. Laser Physics Letters, 2015, 12, 015002.	1.4	15
203	High-Contrast, High-Intensity Petawatt-Class Laser and Applications. IEEE Journal of Selected Topics in Quantum Electronics, 2015, 21, 232-249.	2.9	60
204	Laser-driven high-energy proton beam with homogeneous spatial profile from a nanosphere target. Physical Review Special Topics: Accelerators and Beams, 2015, 18, .	1.8	43
205	Microchip Laser Operation of Yb-Doped Gallium Garnets. , 2015, , .		0
206	Impacts of Ambient and Ablation Plasmas on Short- and Ultrashort-Pulse Laser Processing of Surfaces. Micromachines, 2014, 5, 1344-1372.	2.9	29
207	Short-wavelength ablation of polymers in the high-fluence regime. Physica Scripta, 2014, T161, 014066.	2.5	6
208	Extreme ultraviolet emission and confinement of tin plasmas in the presence of a magnetic field. Physics of Plasmas, 2014, 21, 053106.	1.9	22
209	Tunable mid-IR parametric conversion system pumped by a high-average-power picosecond Yb:YAG thin-disk laser. Proceedings of SPIE, 2014, , .	0.8	1
210	Design of a kJ-class HiLASE laser as a driver for inertial fusion energy. High Power Laser Science and Engineering, 2014, 2, .	4.6	15
211	Design of kJ-class HiLASE laser as a driver for inertial fusion energy – CORRIGENDUM. High Power Laser Science and Engineering, 2014, 2, .	4.6	0
212	EUV ablation of organic polymers at a high fluence. High Power Laser Science and Engineering, 2014, 2,	4.6	0
213	Cryogenic laser performance of Yb:YAG diode-pumped at 940 nm and 969 nm for high power lasers. , 2014, , .		0
214	Design and optimization of an adaptive optics system for a high-average-power multi-slab laser (HiLASE): erratum. Applied Optics, 2014, 53, 7877.	2.1	0
215	Evolution of laser-produced Sn extreme ultraviolet source diameter for high-brightness source. Applied Physics Letters, 2014, 105, 074103.	3.3	11
216	Active wavefront control in Hilase multislab high-average-power laser system. , 2014, , .		1

#	Article	IF	CITATIONS
217	Characterization of diode-laser stacks for high-energy-class solid state lasers. Proceedings of SPIE, 2014, , .	0.8	1
218	High-energy picosecond light source based on cryogenically conduction cooled Yb-doped laser amplifier. Proceedings of SPIE, 2014, , .	0.8	1
219	50-mJ, 1-kHz Yb:YAG thin-disk regenerative amplifier with 969-nm pulsed pumping. , 2014, , .		2
220	Optimization of beam quality and optical-to-optical efficiency of Yb:YAG thin-disk regenerative amplifier by pulsed pumping. Optics Letters, 2014, 39, 1441.	3.3	24
221	Zero-phonon-line pumped 100-kHz Yb:YAG thin disk regenerative amplifier. Proceedings of SPIE, 2014, , .	0.8	2
222	Overview of the HiLASE project: high average power pulsed DPSSL systems for research and industry. High Power Laser Science and Engineering, 2014, 2, .	4.6	43
223	Spectroscopic characterization of Yb3+-doped laser materials at cryogenic temperatures. Applied Physics B: Lasers and Optics, 2014, 116, 75-81.	2.2	70
224	Design and optimization of an adaptive optics system for a high-average-power multi-slab laser (HiLASE). Applied Optics, 2014, 53, 3255.	1.8	18
225	Periodic nanostructures self-formed on silicon and silicon carbide by femtosecond laser irradiation. Applied Physics A: Materials Science and Processing, 2014, 117, 49-54.	2.3	11
226	Efficient ASE Management in Disk Laser Amplifiers With Variable Absorbing Clads. IEEE Journal of Quantum Electronics, 2014, 50, 1-9.	1.9	11
227	Pulsed laser modification of transparent dielectrics: what can be foreseen and predicted by numerical simulations?. Journal of the Optical Society of America B: Optical Physics, 2014, 31, C8.	2.1	35
228	Suppression of nonlinear phonon relaxation in Yb:YAG thin disk via zero phonon line pumping. Optics Letters, 2014, 39, 4919.	3.3	44
229	Periodic Grating Structures on Metal Self-organized by Double-pulse Irradiation. Journal of Laser Micro Nanoengineering, 2014, 9, 234-237.	0.1	20
230	HiLASE: Development of Fully Diode-Pumped, kW-Class Pulsed Lasers for High-Tech Applications. The Review of Laser Engineering, 2014, 42, 145.	0.0	0
231	Development of the estimation method for thermo-optics effects in the TGG ceramics rod. , 2014, , .		0
232	High-power, picosecond pulse thin-disk lasers in the Hilase project. Proceedings of SPIE, 2013, , .	0.8	3
233	Generation of periodic structures on SiC upon laser plasma XUV/NIR radiations. Laser and Particle Beams, 2013, 31, 547-550.	1.0	1
234	Optimization of Wavefront Distortions and Thermal-Stress Induced Birefringence in a Cryogenically-Cooled Multislab Laser Amplifier. IEEE Journal of Quantum Electronics, 2013, 49, 960-966.	1.9	46

#	Article	IF	CITATIONS
235	Spectroscopic characterization of various Yb ³⁺ doped laser materials at cryogenic temperatures for the development of high energy class diode pumped solid state lasers. Proceedings of SPIE, 2013, , .	0.8	13
236	30-mJ, 1-kHz, Yb:YAG thin disk regenerative amplifier with pulsed pumping at 969-nm. , 2013, , .		0
237	1-kHz pulsed pumped Yb:YAG thin disk regenerative amplifier. , 2013, , .		0
238	Evolution of Î ² -SiC in laser-generated plasmas. Applied Surface Science, 2013, 272, 19-24.	6.1	2
239	In-situ optical phase distortion measurement of Yb:YAG thin disk in high average power regenerative amplifier. Proceedings of SPIE, 2013, , .	0.8	2
240	Modeling and optimization of thin disk structure for high power sub-joule laser. , 2013, , .		0
241	HiLASE cryogenically-cooled diode-pumped laser prototype for inertial fusion energy. Proceedings of SPIE, 2013, , .	0.8	7
242	Advantages of zero phonon line pumping in 100kHz Yb:YAG thin-disk regenerative amplifier. , 2013, , .		0
243	Design of a tunable parametric wavelength conversion system between 2 and 3 μm pumped by a high-average-power Yb:YAG thin-disk laser. , 2013, , .		0
244	Experimental test of TOF diagnostics for PW class lasers. Proceedings of SPIE, 2013, , .	0.8	2
245	Effective mid-IR pulse generation pumped by high average power thin disk regenerative amplifier. , 2013, , .		0
246	Zero-phonon-line pumped 1 kHz Yb:YAG thin-disk regenerative amplifier. , 2013, , .		1
247	Enhanced TNSA acceleration with 0.1-1 PW lasers. Proceedings of SPIE, 2013, , .	0.8	2
248	Design of high-energy-class cryogenically cooled Yb3+â^¶YAG multislab laser system with low wavefront distortion. Optical Engineering, 2013, 52, 064201.	1.0	20
249	Simulation of performance of wavefront correction using deformable mirror in high-average-power laser systems. , 2013, , .		6
250	Effect of amplified spontaneous emission and parasitic oscillations on the performance of cryogenically-cooled slab amplifiers. Laser and Particle Beams, 2013, 31, 553-560.	1.0	8
251	Metal-like self-organization of periodic nanostructures on silicon and silicon carbide under femtosecond laser pulses. Journal of Applied Physics, 2013, 114, .	2.5	37
252	Simple measurement of picosecond laser pulses in a wavelength range above $1\hat{l}^{1}\!/\!4$ m. , 2013, , .		0

#	Article	IF	CITATIONS
253	Conceptual design of 100 J cryogenically-cooled multi-slab laser for fusion research. EPJ Web of Conferences, 2013, 59, 08004.	0.3	2
254	Status of HiLASE project: High average power pulsed DPSSL systems for research and industry. EPJ Web of Conferences, 2013, 59, 08003.	0.3	2
255	Development of High Energy and High Average Power Ultrafast Thin Disk Lasers. The Review of Laser Engineering, 2013, 41, 703.	0.0	1
256	New methods for high current fast ion beam production by laser-driven acceleration. Review of Scientific Instruments, 2012, 83, 02B307.	1.3	7
257	High-energy, picosecond regenerative thin-disk amplifier at 1 kHz. Proceedings of SPIE, 2012, , .	0.8	5
258	100-J level amplifier concepts for HiLASE and ELI-Beamlines. , 2012, , .		0
259	High-energy regenerative thin disk amplifier. , 2012, , .		0
260	Modeling of amplified spontaneous emission, heat deposition, and energy extraction in cryogenically cooled multislab Yb^3+:YAG laser amplifier for the HiLASE Project. Journal of the Optical Society of America B: Optical Physics, 2012, 29, 1270.	2.1	45
261	Advanced LIDT testing station in the frame of the HiLASE Project. Proceedings of SPIE, 2012, , .	0.8	2
262	Design and modeling of kW-class thin-disk lasers. Proceedings of SPIE, 2012, , .	0.8	1
263	Comparative design study of 100 J cryogenically cooled Yb:YAG multi-slab amplifiers operating at 10 Hz. , 2012, , .		2
264	Laser-Driven Proton Acceleration Enhancement by Nanostructured Foils. Physical Review Letters, 2012, 109, 234801.	7.8	178
265	Pilot experiment on proton acceleration using the 25 TW femtosecond Ti:Sapphire laser system at PALS. Nuclear Instruments and Methods in Physics Research, Section A: Accelerators, Spectrometers, Detectors and Associated Equipment, 2012, 690, 48-52.	1.6	1
266	Performance of a 100J cryogenically cooled multi-slab amplifier with respect to the pump beam parameters and geometry. Proceedings of SPIE, 2012, , .	0.8	2
267	Full characterization of laser-accelerated ion beams using Faraday cup, silicon carbide, and single-crystal diamond detectors. Journal of Applied Physics, 2011, 109, .	2.5	68
268	Advances in laser driven soft x-ray lasers at LOA. Proceedings of SPIE, 2011, , .	0.8	0
269	25TW Ti:sapphire laser chain at PALS. Proceedings of SPIE, 2011, , .	0.8	10
270	Numerical evaluation of heat deposition in cryogenically cooled multi-slab amplifier. Proceedings of SPIE, 2011, , .	0.8	0

#	Article	IF	CITATIONS
271	Efficient surface processing by ultrafast XUV/NIR dual action. , 2011, , .		О
272	Beam properties of fully optimized, table-top, coherent source at 30 nm. Opto-electronics Review, 2011, 19, .	2.4	2
273	High energy density matter generation using a focused soft-X-ray laser for volumetric heating of thin foils. High Energy Density Physics, 2011, 7, 11-16.	1.5	2
274	Enhanced surface structuring by ultrafast XUV/NIR dual action. New Journal of Physics, 2011, 13, 053049.	2.9	7
275	Outline of the ELI-Beamlines facility. Proceedings of SPIE, 2011, , .	0.8	17
276	Characterization of a seeded optical-field ionized collisional soft x-ray laser. Springer Proceedings in Physics, 2011, , 127-135.	0.2	0
277	Bessel spatial profile of a soft x-ray laser beam. Applied Physics Letters, 2010, 97, .	3.3	3
278	Preliminary studies on fast particle diagnostics for the future fs-laser facility at PALS. Radiation Effects and Defects in Solids, 2010, 165, 419-428.	1.2	0
279	Ablative microstructuring with plasma-based XUV lasers and efficient processing of materials by dual action of XUV/NIR–VIS ultrashort pulses. Radiation Effects and Defects in Solids, 2010, 165, 551-558.	1.2	4
280	Observation of spectral gain narrowing in a high-order harmonic seeded soft-x-ray amplifier. Physical Review A, 2010, 81, .	2.5	18
281	Investigations of laser-induced damages in fused silica optics using x-ray laser interferometric microscopy. Journal of Applied Physics, 2010, 107, .	2.5	9
282	Measurements of the highest acceleration gradient for ions produced with a long laser pulse. Review of Scientific Instruments, 2010, 81, 02A506.	1.3	16
283	Measuring the electron density gradients of dense plasmas by deflectometry using short-wavelength probe. Physics of Plasmas, 2010, 17, 122705.	1.9	11
284	Fourier-limited seeded soft x-ray laser pulse. Optics Letters, 2010, 35, 1326.	3.3	22
285	Experimental study of radiative shocks at PALS facility. Laser and Particle Beams, 2010, 28, 253-261.	1.0	21
286	Surface modification of organic polymer by dual action of extreme ultraviolet/visible-near infrared ultrashort pulses. Journal of Applied Physics, 2009, 105, 026105.	2.5	11
287	Filamented plasmas in laser ablation of solids. Plasma Physics and Controlled Fusion, 2009, 51, 035013.	2.1	11
288	Research on the seeding of high-energy harmonic pulse into an x-ray lasing medium. , 2009, , .		0

#	Article	IF	CITATIONS
289	Experimental investigation of fast electron transport in solid density matter: Recent results from a new technique of X-ray energy-encoded 2D imaging. Laser and Particle Beams, 2009, 27, 643-649.	1.0	4
290	Measurements of opacity and temperature of warm dense matter heated by focused soft X-ray laser irradiation. High Energy Density Physics, 2009, 5, 110-113.	1.5	5
291	Plasma-based X-ray laser at 21Ânm for multidisciplinary applications. European Physical Journal D, 2009, 54, 439-444.	1.3	6
292	Aberration-free laser beam in the soft x-ray range. Optics Letters, 2009, 34, 2438.	3.3	36
293	Applications of high energy X-ray lasers in plasma probing and warm dense matter generation. , 2009, , .		0
294	Laser-induced damage studies in optical elements using X-ray laser interferometric microscopy. Proceedings of SPIE, 2009, , .	0.8	1
295	Efficient materials processing by dual action of XUV/Vis-NIR ultrashort laser pulses. , 2009, , .		0
296	Damage thresholds of various materials irradiated by 100-ps pulses of 21.2-nm laser radiation. , 2009, , .		0
297	Improved efficiency of materials processing by dual action of XUV/Vis-NIR ultrashort laser pulses and comprehensive study of high-order harmonic source at PALS. , 2009, , .		0
298	High Resolution X-Ray Laser Backlighting of Plasmas Using Spatial Filtering Technique. Springer Proceedings in Physics, 2009, , 417-425.	0.2	5
299	Characterization of focused beam of desktop 10-Hz capillary-discharge 46.9-nm laser. Proceedings of SPIE, 2009, , .	0.8	8
300	Innershell X-Ray Laser in Sodium Vapor: Final Steps Towards Experimental Verification. Springer Proceedings in Physics, 2009, , 557-562.	0.2	0
301	Highly Efficient Surface Modification of Solids by Dual Action of XUV/Vis-NIR Laser Pulses. Springer Proceedings in Physics, 2009, , 401-407.	0.2	1
302	Single-shot soft x-ray laser-induced ablative microstructuring of organic polymer with demagnifying projection. Optics Letters, 2008, 33, 1087.	3.3	14
303	Development of ultrafast soft x-ray beamline based on high-order harmonic generation at PALS. , 2008, , .		0
304	Generation of submicrojoule high harmonics using a long gas jet in a two-color laser field. Applied Physics Letters, 2008, 92, .	3.3	106
305	Development of ultrafast soft x-ray beamline at PALS and surface modification of solids by high-order harmonics. Proceedings of SPIE, 2007, 6702, 240.	0.8	0
306	Laser-Ablation Rates Measured Using X-Ray Laser Transmission. Physical Review Letters, 2007, 99, 195002.	7.8	19

#	Article	IF	CITATIONS
307	Applications of a 10-mJ soft X-ray laser: from dense plasma physics to micro-structuring. , 2007, , .		Ο
308	Multidisciplinary Applications of Highly Energetic Soft X-Ray Laser at 21 nm. Conference Proceedings - Lasers and Electro-Optics Society Annual Meeting-LEOS, 2007, , .	0.0	0
309	21-nm x-ray laser Thomson scattering of laser-heated exploding foil plasmas. Proceedings of SPIE, 2007, , .	0.8	0
310	Utilizing ablation of solids to characterize a focused soft X-ray laser beam. , 2007, , .		6
311	Development of soft x-ray lasers at PALS and their applications in dense plasma physics. Proceedings of SPIE, 2007, , .	0.8	1
312	X-ray lasers as probes to measure plasma ablation rates. Proceedings of SPIE, 2007, , .	0.8	1
313	Demonstration of a spatial filtering amplifier for high-order harmonics. Optics Letters, 2007, 32, 1498.	3.3	20
314	Development and applications of multimillijoule softX-ray lasers. Journal of Modern Optics, 2007, 54, 2571-2583.	1.3	7
315	High Pressure Laser-Generated Shocks and Application to EOS of Carbon. Journal of Physics: Conference Series, 2007, 71, 012001.	0.4	4
316	Effect of lateral radiative losses on radiative shock propagation. High Energy Density Physics, 2007, 3, 8-11.	1.5	15
317	High-pressure behavior of carbon by laser-generated shocks. Russian Journal of Physical Chemistry A, 2007, 81, 1360-1364.	0.6	0
318	Determination of the Ion Temperature in a Plasma Created by Optical Field Ionization. Contributions To Plasma Physics, 2007, 47, 352-359.	1.1	6
319	Focusing a multimillijoule soft x-ray laser at 21nm. Applied Physics Letters, 2006, 89, 051501.	3.3	28
320	Exposed sets in potential theoryâ~†â~†The work is part of the research project MSM 0021620839 financed by MSMT Bulletin Des Sciences Mathematiques, 2006, 130, 646-659.	1.0	0
321	Homogeneous focusing with a transient soft X-ray laser for irradiation experiments. Optics Communications, 2006, 263, 98-104.	2.1	5
322	Second generation X-ray lasers. Journal of Quantitative Spectroscopy and Radiative Transfer, 2006, 99, 142-152.	2.3	7
323	Plasma Based X-ray Lasers Used For Opacity and Ablation Rate Measurements. AIP Conference Proceedings, 2006, , .	0.4	0
324	Astrophysical radiative shocks: From modeling to laboratory experiments. Laser and Particle Beams, 2006, 24, 535-540.	1.0	34

#	Article	IF	CITATIONS
325	Characterization of the collisionally pumped optical-field-ionized soft-x-ray laser at41.8nmdriven in capillary tubes. Physical Review A, 2006, 73, .	2.5	36
326	Opacity Measurements of a Hot Iron Plasma Using an X-Ray Laser. Physical Review Letters, 2006, 97, 035001.	7.8	32
327	Laser X-UV en schéma collisionnel OFI à 41,8 nm créé dans des tubes capillaires. European Physical Journal Special Topics, 2006, 138, 43-53.	0.2	Ο
328	Microscopie interférentielle X-UVÂ: un outil pour l'étude des endommagements des surfaces optiques. European Physical Journal Special Topics, 2006, 138, 245-250.	0.2	0
329	Development of soft x-ray lasers at PALS. , 2005, , .		1
330	Advanced optical damage studies using x-ray laser interferometric microscopy. , 2005, , .		2
331	Development and applications of 10-mJ x-ray lasers at PALS. , 2005, , .		0
332	Soft X-ray laser of second generation. , 2005, , .		0
333	Nanometric deformations of thin Nb layers under a strong electric field using soft x-ray laser interferometry. Journal of Applied Physics, 2005, 98, 044308.	2.5	6
334	Progress in optical-field-ionization soft X-ray lasers at LOA. Laser and Particle Beams, 2005, 23, .	1.0	7
335	Absolute Time-Resolved X-Ray Laser Gain Measurement. Physical Review Letters, 2005, 95, 173902.	7.8	31
336	Dramatic enhancement of xuv laser output using a multimode gas-filled capillary waveguide. Physical Review A, 2005, 71, .	2.5	26
337	Lasers collisionnels à 41.8 nm en régime guidé. European Physical Journal Special Topics, 2005, 127, 33-37.	0.2	0
338	Lasers X de deuxième génération. European Physical Journal Special Topics, 2005, 127, 9-13.	0.2	0
339	Hugoniot Data for Carbon at Megabar Pressures. Physical Review Letters, 2004, 92, 065503.	7.8	41
340	41.8â^'nmXe8+laser driven in a plasma waveguide. Physical Review A, 2004, 70, .	2.5	12
341	A high-intensity highly coherent soft X-ray femtosecond laser seeded by a high harmonic beam. Nature, 2004, 431, 426-429.	27.8	313
342	Progress on Collisionally Pumped Optical-Field-Ionization Soft X-Ray Lasers. IEEE Journal of Selected Topics in Quantum Electronics, 2004, 10, 1351-1362.	2.9	1

#	Article	IF	CITATIONS
343	Soft X-ray contact microscopy of nematode Caenorhabditis elegans. European Physical Journal D, 2004, 30, 235-241.	1.3	8
344	Laser driven shock experiments at PALS. European Physical Journal D, 2004, 54, C431-C443.	0.4	2
345	Characterization of collisionally pumped optical-field-ionization soft X-ray lasers. Applied Physics B: Lasers and Optics, 2004, 78, 939-944.	2.2	10
346	X-ray microscopy and imaging of Caenorhabditis elegans nematode using a laser-plasma-pulsed x-ray source. , 2004, , .		0
347	<title>Laser-driven shock experiments at PALS</title> ., 2004, , .		0
348	<title>Carbon hugoniot at megabar pressures driven by laser-induced shocks</title> ., 2004, , .		0
349	Study of the stability of beam characteristics of the neon-like Zn X-ray laser using a half cavity. European Physical Journal D, 2003, 22, 31-40.	1.3	10
350	Statistical investigations of the beam stability of the double-pass amplified zinc soft X-ray laser at 21.2 nm. European Physical Journal D, 2003, 26, 59-65.	1.3	1
351	Choquet like sets in function spaces. Bulletin Des Sciences Mathematiques, 2003, 127, 397-437.	1.0	5
352	Demonstration of a Collisionally Excited Optical-Field-Ionization XUV Laser Driven in a Plasma Waveguide. Physical Review Letters, 2003, 91, 205001.	7.8	74
353	Investigations of collisionally pumped optical field ionization soft-x-ray lasers. Journal of the Optical Society of America B: Optical Physics, 2003, 20, 195.	2.1	14
354	Beam properties of a deeply saturated, half-cavity zinc soft-x-ray laser. Journal of the Optical Society of America B: Optical Physics, 2003, 20, 1386.	2.1	14
355	Shock pressure induced by 0.44 μm laser radiation on aluminum targets. Laser and Particle Beams, 2003, 21, 481-487.	1.0	18
356	X-ray microscopy of living multicellular organisms with the Prague Asterix Iodine Laser System. Laser and Particle Beams, 2003, 21, 511-516.	1.0	8
357	Prague Asterix Laser System (PALS) - results and upgrades. , 2003, 5228, 651.		1
358	Ablation pressure scaling at short laser wavelength. Physical Review E, 2003, 68, 067403.	2.1	53
359	Observation of enhanced soft x-ray emission using nitrogen clusters ionized by intense, femtosecond laser. Journal of Applied Physics, 2003, 93, 3105-3107.	2.5	1
360	Advances in collisionally pumped optical-field-ionization soft x-ray lasers. , 2003, 5197, 119.		2

#	Article	IF	CITATIONS
361	Demonstration of lasing at 41.8 nm in Xe8+driven in a plasma waveguide. , 2003, , .		Ο
362	Lasers XUV collisionnels pompés par des lasers femtoseconde. European Physical Journal Special Topics, 2003, 108, 161-164.	0.2	0
363	Demonstration of a Ni-Like Kr Optical-Field-Ionization Collisional Soft X-Ray Laser at 32.8Ânm. Physical Review Letters, 2002, 89, 253901.	7.8	91
364	Investigation of soft X-ray emission from Ar clusters heated by ultrashort laser pulses. Laser and Particle Beams, 2002, 20, 51-57.	1.0	2
365	Development and applications of X-ray lasers at LSAI/LIXAM. AIP Conference Proceedings, 2002, , .	0.4	0
366	Multimillijoule, highly coherent x-ray laser at 21 nm operating in deep saturation through double-pass amplification. Physical Review A, 2002, 66, .	2.5	110
367	Multi-millijoule, deeply saturated x-ray laser at 21.2 nm for applications in plasma physics. Plasma Physics and Controlled Fusion, 2002, 44, B207-B223.	2.1	11
368	<title>X-ray laser progress for applications</title> ., 2001, 4505, 211.		0
369	The Prague Asterix Laser System. Physics of Plasmas, 2001, 8, 2495-2501.	1.9	259
370	<title>Soft x-ray emission from Ar clusters heated by ultrashort laser pulse</title> ., 2001, , .		0
371	<title>Investigation of soft x-ray emission in the water window for microscopy using a double-stream gas puff target irradiated with the Prague Asterix Laser System (PALS)</title> ., 2001, , .		6
372	<title>Intensity distribution of the focal lines of the prepulse and mainpulse at the solid target surface</title> ., 2001, 4424, 561.		0
373	<title>Collisional optical-field ionization soft x-ray lasers</title> . , 2001, 4505, 195.		3
374	X-ray laser facility at the PALS centre. European Physical Journal Special Topics, 2001, 11, Pr2-589-Pr2-596.	0.2	2
375	Investigations on femtosecond-pulse-driven soft X-ray lasers using a gas puff target irradiated with a Ti:Sapphire laser. European Physical Journal Special Topics, 2001, 11, Pr2-197-Pr2-200.	0.2	0
376	Intensity distribution of the focal lines of the prepulse and mainpulse at the solid target surface. European Physical Journal Special Topics, 2001, 11, Pr2-601-Pr2-604.	0.2	0
377	Interaction of intense, femtosecond laser pulse with small-sized Ne clusters. European Physical Journal Special Topics, 2001, 11, Pr2-433-Pr2-436.	0.2	0
378	Soft-x-ray emission from small-sized Ne clusters heated by intense, femtosecond laser pulses. Physical Review E, 2000, 62, 4461-4464.	2.1	13

#	Article	IF	CITATIONS
379	Enhancement of soft x-ray emission from a cryogenically cooled Ar gas jet irradiated by 25 fs laser pulse. Applied Physics Letters, 2000, 76, 1819-1821.	3.3	30
380	Investigation of Zn and Cu prepulse plasmas relevant to collisional excitation x-ray lasers. Physical Review A, 1997, 56, 4229-4241.	2.5	31
381	Electron density profile measurements of line plasmas by interferometric technique. , 1996, 2767, 119.		0
382	Experimental investigation of line plasmas created by intensities 109- 1011Wcm-2. , 1996, , .		1
383	lodine laser production of highly charged Ta ions. European Physical Journal D, 1996, 46, 1099-1115.	0.4	31
384	Thomson parabola ion spectrograph with the microchannel plate image converter in investigations of highâ€Z laser plasma ion sources. Review of Scientific Instruments, 1996, 67, 1272-1274.	1.3	18
385	Design of efficient soft X-ray laser using neonlike Fe driven by iodine laser. , 1996, , .		0
386	Influence of laser-beam focusing on the production of highly charged ions from laser plasma. , 1996, ,		1